DOI 10.1007/s11182-016-0899-0

Russian Physics Journal, Vol. 59, No. 8, December, 2016 (Russian Original No. 8, August, 2016)

THE MECHANISM OF ORIENTATION DEPENDENCE OF CYCLIC STABILITY OF SUPERELESTICITY IN NiFeGaCo SINGLE CRYSTALS UNDER COMPRESSION

E. E. Timofeeva,[1] E. Yu. Panchenko,[1]
N. G. Vetoshkina,[1] Yu. I. Chumlyakov,[1]
A. I. Tagiltsev,[1] A. S. Eftifeeva,[1] and H. Maier[2]

UDC 669.24'1'871-539.371:548.55

Using single crystals of the $Ni_{49}Fe_{18}Ga_{27}Co_6$ *(at.%) alloy, oriented along [001]- and [123]-directions, cyclic stability of superelasticity is investigated in isothermal loading/unloading cycles at* $T = A_f + (12–15)$ *K (100 cycles) under compressive stress as a function of given strain per cycle, presence of disperse γ-phase particles measuring 5–10 μm, austenitic (B2 or* $L2_1$*) and stress-induced martensitic crystal structure (14M or* $L1_0$*). It is shown that single-phase* $L2_1$*-crystals demonstrate high cyclic stability during* $L2_1$*–14M-transitions with narrow hysteresises* $\Delta\sigma < 50$ *MPa in the absence of detwinning of the martensite. During the development of* $L2_1$*–14M stress-induced transformation, the reversible energy* ΔG_{rev} *for these crystals exceeds the dissipated energy* ΔG_{irr}*, and* $\Delta G_{rev}/\Delta G_{irr} = 1.7–1.8$*. A significant degradation of superelasticity is observed in [123]-oriented crystals during the development of* $L2_1$*–14M–*$L1_0$*-transformations followed by detwinning of the* $L1_0$*-martensite crystals and heterophase (B2+γ) single crystals, irrespective of their orientation during the B2–*$L1_0$*-transition. In the latter case, martensitic transformations are characterized by a wide stress hysteresis* $\Delta\sigma \geq 80$ *MPa and the dissipated energy exceeds the reversible energy* $\Delta G_{rev}/\Delta G_{irr} = 0.5$*. The empirical criterion, relying on the analysis of the reversible-to-irreversible energy ratio,* $\Delta G_{rev}/\Delta G_{irr}$*, during stress-induced martensitic transformations, can be used to predict the cyclic stability of superelasticity in* NiFeGaCo *alloys subjected to different types of heat treatment.*

Keywords: superelasticity, cyclic stability, thermoelastic martensitic transformations, single crystals, stress hysteresis.

INTRODUCTION

Nickel-base ferromagnetic Heusler alloys with a shape-memory effect have been intensively investigated for the recent twenty years. Their principal feature is a possibility of controlling the austenite – martensite phase transition not only via temperature and mechanical stress variations but also using a magnetic field. Nickel-base Heusler alloys (NiMnGa, NiFeGa(Co), NiMnInCo) exhibit high-temperature superelasticity (SE) up to 400°C, very large field-induced strains up to 10%, and magneto- and elastocaloric effects [1–3]. These multifunctional materials offer new practical solutions due to multiple transformations of the magnetic and thermal energies into mechanical work and vice versa. One of the principal factors, preventing their extensive application in multi-shot reclosing relays, is the low cyclic stability of their functional properties. Today, the investigations dealing with microstructural mechanisms of

[1]V. D. Kuznetsov Siberian Physical Technical Institute at Tomsk State University, Tomsk, Russia, e-mail: katie@sibmail.com; panchenko@mail.tsu.ru; vetoshkina23011991@mail.ru; chum@phys.tsu.ru; antontgl@gmail.com; anna_eftifeeva@rambler.ru; [2]Institut für Werkstoffkunde, Leibniz Universität Hannover, Garbsen, Germany, e-mail: maier@iw.uni-hannover.de. Translated from Izvestiya Vysshikh Uchebnykh Zavedenii, Fizika, No. 8, pp. 114–122, August, 2016. Original article submitted May 24, 2016.

TABLE 1. Theoretical Values of Transformation Strain for NiFeGa(Co) Single Crystals [7]

MT type	$L2_1$–14M		$L2_1(B2)$–$L1_0$	
Orientation	[001]	[123]	[001]	[123]
ε_{CVP},%	6.03	3.63	6.25	3.79
$\varepsilon_{CVP+detw}$,%	6.38	3.72	6.25	4.77

degradation and methods for improving the stability of thermomechanical properties of Heusler Ni-base alloys are few [4–6]. It is shown in [5] that NiFeGa single-phase crystals demonstrate a strong orientation dependence of cyclic stability of SE under tensile stress. Single crystals oriented along the [001]-direction in the case of 3% given strain withstand up to 18 000 loading/unloading cycles during SE without significant degradation and exhibit high cyclic stability: neither the values of critical stresses of martensite formation σ_{cr} nor that of stress hysteresis $\Delta\sigma$ depend on the number of loading/unloading cycles, and there is no increase in the irreversible strain ε_{irr}, while the [123]-oriented crystals fail after 60 cycles [5]. There are no answers to the physical reasons for the strong orientation dependence, the microstructural mechanisms of degradation, the influence of the level of given strain per cycle, the sequence of martensitic transformations (MTs) and the influence of the disperse second-phase particles on the cyclic stability in these crystals so far. Without investigations providing the answers to these questions, it is impossible to predict the stability of functional properties to cyclic stress. The purpose of this work is to study the orientation dependence of cyclic stability of SE under tensile stress of $Ni_{49}Fe_{18}Ga_{27}Co_6$ (at.%) single- and heterophase single crystals oriented along [001]- and [123]-directions.

In order to determine the influence of crystal structure of stress-induced martensite (14M, $L1_0$) and γ-phase particles on cyclic stability of SE, we primarily selected $Ni_{49}Fe_{18}Ga_{27}Co_6$ as-grown single crystals in one-phase with the $L2_1$-structure [3, 6]. It was shown in our previous work [3] and in [7] that in $L2_1$-NiFeGa(Co) single crystals in compression within the temperature interval $T < 340$–370 K an $L2_1$–14M-MT occurs in the [001]-orientation. In other orientations ([011], [012]), there is a sequence of $L2_1$–14M–$L1_0$-MTs. Secondly, we took $Ni_{49}Fe_{18}Ga_{27}Co_6$ single crystals after thermal treatment: heating to 1373 K, which is higher than the order – disorder transition temperature (~923–973 K [8]), annealing for 25 min and quenching into water. After quenching, the crystals contain γ-phase particles (length 5–10 μm, volume fraction ~7%) [9] and undergo a stress-induced $B2$–$L1_0$-MT.

The choice of [001]- and [123]-orientations of single crystals for the present investigations of orientation dependence of SE cyclic stability relies on the analysis of theoretical calculations of transformation strain using the theory of energy minimization during the formation of twinned martensite ε_{CVP} and its subsequent detwinning $\varepsilon_{CVP+detw}$ [7]. It is evident from Table 1 that the contribution from the 14M-martensite detwinning into transformation strain approximates zero irrespective of crystal orientations. If the $L1_0$-martensite does not detwin during a stress-induced MT, then the values of transformation strain during the formation of 14M- and $L1_0$-structures are close $\varepsilon_{CVP}^{L1_0} \approx \varepsilon_{CVP+detw}^{14M}$, which is observed in [001]-oriented single crystals. In [123]-oriented single crystals, detwinning of $L1_0$-martensite contributes into the transformation strain and $\varepsilon_{CVP+detw}^{L1_0} > \varepsilon_{CVP}^{L1_0} = \varepsilon_{CVP+detw}^{14M}$. As it follows from [10, 11], during detwinning the habitus plane moves from its invariant undistorted position, which gives rise to development of internal stresses, increases energy dissipation during MTs, and can favor SE degradation.

1. EXPERIMENTAL PROCEDURE

Single crystals of the $Ni_{49}Fe_{18}Ga_{27}Co_6$ (at.%) alloy were grown using the Bridgeman process. The specimens oriented along [001]- and [123]-directions for compressive tests were shaped as parallelepipeds measuring 2.8×2.8×6 mm. Orientation dependence of their cyclic stability was investigated in two structural states: 1) after growth without any additional heat treatment ($L2_1$-crystals); and 2) after annealing at 1373 K for 25 min, followed by quenching into water ($B2$+γ)-crystals). Isothermal loading/unloading cycling (100 cycles) was performed at the

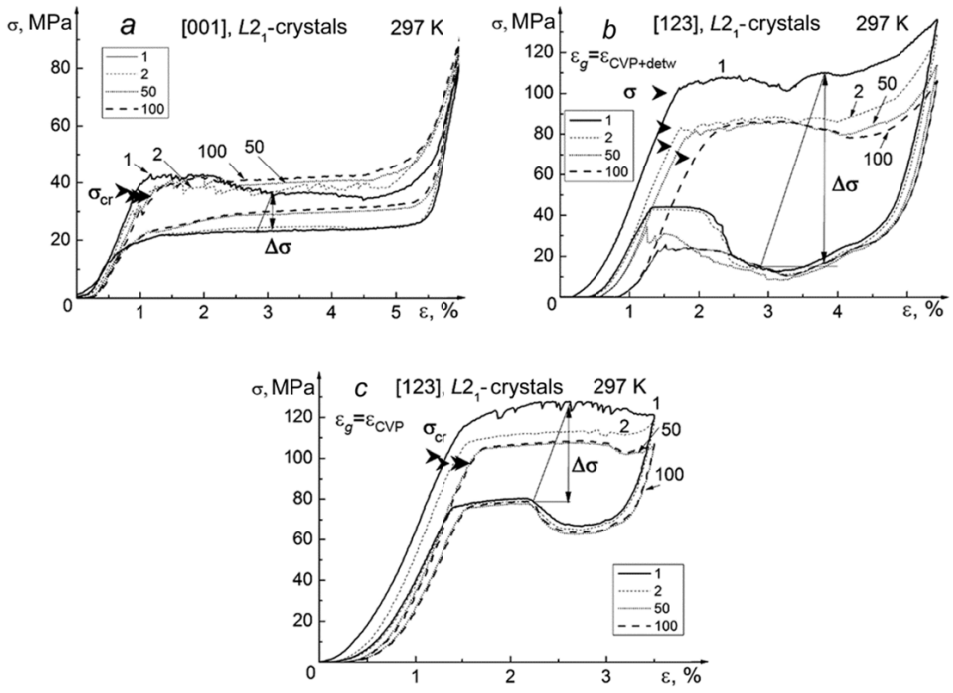

Fig. 1. Results of cyclic testing of $L2_1$-crystals of $Ni_{49}Fe_{18}Ga_{27}Co_6$ alloy: [001]-orientation at $\varepsilon_g = 6.0\%$ (*a*), [123]-orientation at $\varepsilon_g = 3.5\%$ (*b*), and [123]-orientation at $\varepsilon_g = 5.5\%$ (*c*).

temperature $T = A_f$+(12–15) K in an Instron VHS 5969 universal testing machine at the strain rate $d\varepsilon/dt = 1 \cdot 10^{-3}$ s^{-1}. The MT temperatures, M_s, M_f, A_s and A_f, which were determined from the temperature dependence of electrical conductance, do not depend on orientation and are found to be $M_s = 273$ (±2) K, $M_f = 272$ (±2) K, $A_s = 281$ (±2) K, $A_f = 285$ (±2) K in $L2_1$-crystals and $M_s = 299$ (±2) K, $M_f = 276$ (±2) K, $A_s = 297$ (±2) K, $A_f = 318$ (±2) K in ($B2$+γ)-crystals. Microstructure of the single crystals was examined in a Philips CM 200 transmission electron microscope. Cyclic stability of SE was investigated in two cases: 1) when in [123]-oriented crystals there was no contribution from detwinning into the transformation strain and the value of given strain ε_g corresponded to the formation of 14*M*-martensite or CVP-structure of $L1_0$-martensite, $\varepsilon_g = \varepsilon_{CVP+detw}(14M) = \varepsilon_{CVP}(L1_0) = 3.5$–4%; and 2) when the given strain ε_g in [123]-crystals corresponded to that in a detwinned crystal of $L1_0$-martensite, $\varepsilon_g = 5.5\% \sim \varepsilon_{CVP+detw}(L1_0)$ (the given strain includes elastic strain before MT and reversible transformation strain). The given strain value was not changed in any cycle. Strength properties of the austenite were estimated from the values of critical stress σ_{cr} at the temperature $T = M_d$, where the stresses of martensite formation are consistent with the austenite yield stress.

2. EXPERIMENTAL RESULTS AND DISCUSSION

Figures 1 and 2 present the results of cyclic testing of the initial $L2_1$-crystals of the $Ni_{49}Fe_{18}Ga_{27}Co_6$ alloy during SE (100 loading/unloading cycles at $T = A_f$+12 K = + 297 K), which demonstrate strong orientation dependence of the critical stresses of martensite formation σ_{cr}, the value of stress hysteresis $\Delta\sigma$, and SE cyclic stability. In the [001]-oriented $L2_1$-crystals, a very high SE cyclic stability is obtained and stress-induced MTs are characterized by a narrow stress hysteresis $\Delta\sigma = 12$ MPa and a low stress of martensite formation $\sigma_{cr} < 40$ MPa, whose values remain constant within the measurement error 5% (Fig. 2). A sufficiently high stability is demonstrated by $L2_1$-crystals oriented along the [123]-direction at the low given strain $\varepsilon_g = 3.5\% \sim \varepsilon_{CVP+detw}(14M) = \varepsilon_{CVP}(L1_0)$: with an increase in the number of cycles the critical stresses of martensite formation σ_{cr} decrease by 10%, $\Delta\sigma$ sharply decreases after the first loading/unloading cycle, while from the 2-nd to the 100-th cycle both $\Delta\sigma$ and σ_{cr} remain practically unchanged. It

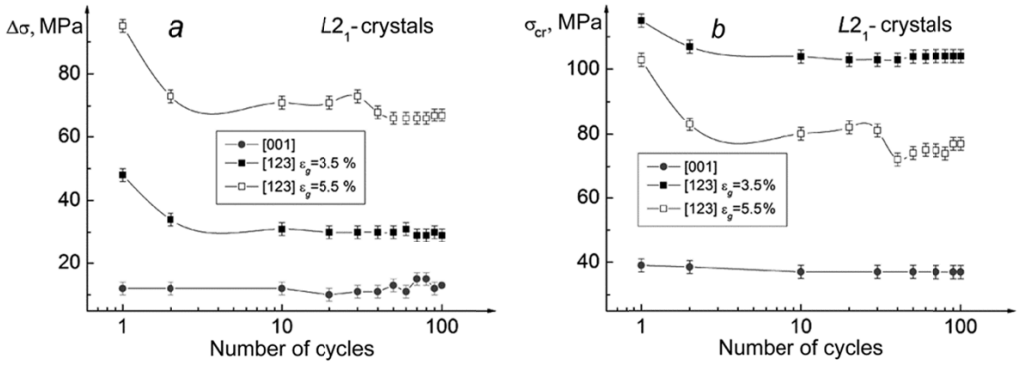

Fig. 2. Depenence of the value of stress hysteresis Δσ (*a*) and critical stress of martensite formation σ_{cr} (*b*) on the number of loading/unloading cycles for $L2_1$-single crystals of $Ni_{49}Fe_{18}Ga_{27}Co_6$ alloy.

should be noted that the values of critical stress, σ_{cr} = 112 MPa, and stress hysteresis, Δσ = 50 MPa, in [123]-oriented crystals are more than twice higher compared with [001]-oriented crystals. In this case, the orientation dependence of critical stress σ_{cr} is controlled by the differing values of Schmidt's factor for respective shear systems during $L2_1$–14*M*-MTs: 0.25 – in [123]-oriented crystals and 0.5 – in [001]-oriented crystals. As the given strain is increased to ε_g = 5.5% ~ $\varepsilon_{CVP+detw}(L1_0)$, the development of stress-induced MTs in [123]-oriented crystals is accompanied by a wide stress hysteresis up to 100 MPa, and dramatic degradation of SE takes place when the number of cycles increases from 1 to 100: the values of σ_{cr} and Δσ decrease by 25 and 30%, respectively, and approximately 1% of irreversible strain is stored (Figs. 1 and 2).

Such a strong dependence of the SE cyclic stability, the values of stress hysteresis $\Delta\sigma$ and critical resolved stresses σ_{cr} on the orientation of $L2_1$-crystals of $Ni_{49}Fe_{18}Ga_{27}Co_6$ alloy and on the value of given strain in the loading/unloading cycle is determined by the difference in the crystal structure of stress-induced martensite, strength properties of the austenitic and martensitic phases, and presence of detwinning of the $L1_0$-martensite crystals.

Firstly, high cyclic stability of SE is observed in $L2_1$-crystals oriented along [001] - and [123]-directions at the given strain $\varepsilon_g = \varepsilon_{CVP+detw}(14M)$, i.e., during stress-induced $L2_1$–14*M*-MTs only. It is well known [12] that 14*M*-martensite contains a high density of twins and does not detwin under stress. This provides high phase-boundary coherence and mobility and determines a low level of energy dissipation during $L2_1$–14*M*-MT and hence a narrow stress hysteresis Δσ. At larger given strain ε_g = 5.5% ~ $\varepsilon_{CVP+detw}(L1_0)$ in $L2_1$-crystals oriented along the [123]-direction a sequence of $L2_1$–14*M*–$L1_0$-MTs takes place, and a complete detwinning of the crystals of $L1_0$-martensite is possible. This implies that the formation of $L1_0$-martensite and its detwinning under stress could be one of the reasons for a low cyclic stability and a wide stress hysteresis in [123]-oriented crystals.

Secondly, when discussing the resistance of shape memory alloys to phase hardening and degradation of their functional properties, we generally take into consideration the austenite strength properties only, since martensitic crystals, containing a large number of twins, exhibit high strength properties and are not plastically deformed during MTs. On the other hand, using [012]-oriented single crystals of NiFeGa alloys under compressive stress, it was shown that martensite can demonstrate low strength properties, and the yield stress level of martensite can be achieved during stress-induced MTs in the case of SE [13]. Therefore in this work for the analysis of the orientation dependence of SE cyclic stability, we consider not only strength properties of the high-temperature $L2_1$-phase, but also those of 14*M*- and $L1_0$-martensites. The [001]-direction is a high-strength orientation: the yield stress level of $L2_1$-phase, σ_{cr}^{A}, exceeds 1000 MPa at T = 800 K, for the 14*M* martensitic phase σ_{cr}^{M} = 1680 MPa at T = 297 K (Fig. 3*a*). Therefore, in [001]-single crystals SE develops at low axial stresses σ_{cr} that are by a factor of 40 lower than the martensite yield stress at the temperature $T = A_f$+12 K = 297 K (Fig. 3*a*). Thus, the development of $L2_1$–14*M*-MTs in the absence of martensite detwinning and in the case of high strength properties of both austenite and martensite ensures high cyclic stability of SE in $L2_1$-crystals oriented along the [001]-direction. Electron microscopy examinations of the specimens after plastic

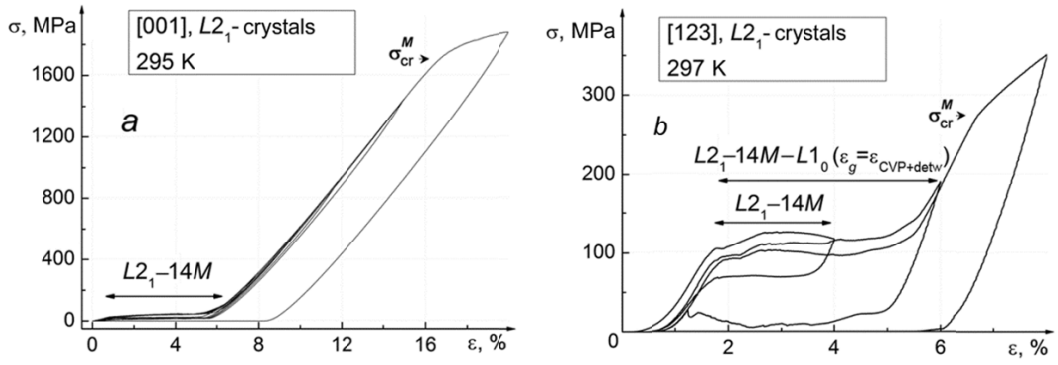

Fig. 3. Curves of σ(ε) response obtained during investigation of the martensite yield stress level in $L2_1$-crystals of $Ni_{49}Fe_{18}Ga_{27}Co_6$ alloy at $T = 297$ K: [001]- (*a*) and [123]- (*b*) orientations.

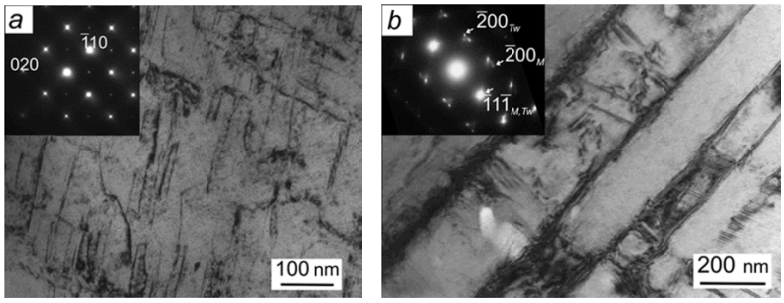

Fig. 4. Microstructure of $L2_1$-single crystals of $Ni_{49}Fe_{18}Ga_{27}Co_6$ alloy after investigations of the martensite yield stress at 297 K: [001]-orientation, $\varepsilon_{irr} = 2\%$, zone axis $[001]_{L21}$(*a*), [123]-orientation, $\varepsilon_{irr} = 3.0\%$, zone axis $[011]_{L10}$ (*b*).

deformation in a martensitic state (at $\sigma > \sigma_{cr}^{M} = 1680$ MPa) at $T = A_f + 12$ K = 297 K reveal the presence of dislocations in the $L2_1$ high-temperature phase, which are inherited by the austenite during a reverse MT (Fig. 4*a*). The reverse MT can occur during heating in the course of foil preparation, without any residual martensite observed in the latter case.

The [123]-orientation in $L2_1$single-phase crystals can be characterized as low-strength orientation, in contrast to [001]: the austenite yield stress level, $\sigma_{cr}^{A} \approx 700$ MPa, is achieved at the temperature $T \sim 700$ K, the martensite strength properties at $T = A_f + 12$ K = 297 K are very low, and the stabilization of $L1_0$-martensite crystals occurs at the external stress equal to 270 MPa (Fig. 3b). Electron microscopy examination of the [123]-oriented crystals tested at $\sigma > \sigma_{cr}^{M} = 270$ MPa reveals the presence of twinned $L1_0$-martensite along the $\{111\}_{L10}$ –planes (Fig. 4*b*), with the twin boundaries stabilized by dislocations.

Thus, $L2_1$-crystals oriented along the [123]-direction at $\varepsilon_g = 5.5\% \sim \varepsilon_{CVP+detw}(L1_0)$ under the conditions of $L1_0$-martensite detwinning in the case of low strength properties of austenite and martensite demonstrate low cyclic stability. On the other hand, if the given strain in [123]-oriented crystals is low and there are no detwinning processes, $\varepsilon_g = 3.5\% \sim \varepsilon_{CVP+detw}(14M) = \varepsilon_{CVP}(L1_0)$, the SE is more stable at the same level of the martensite strength properties.

Figures 5 and 6 present the data of cyclic testing of heterophase ($B2+\gamma$)-crystals at $T = A_f + 15$ K = 333 K.

Unlike $L2_1$-crystals, in ($B2+\gamma$)-crystals, there is a different sequence of stress-induced MTs: high-temperature $B2$-phase transforms into $L1_0$-martensite without any intermediate layered structures, irrespective of orientation [15]. The particles of γ-phase measuring 5–10 μm, which are not observed in the single-phase $L2_1$ single-crystals, during development of a stress-induced MT favor nucleation of a few martensite variants near the particle – matrix interface, which differ from the primary martensite variant with the maximum value of Schmidt's factor. As a result, a multi-

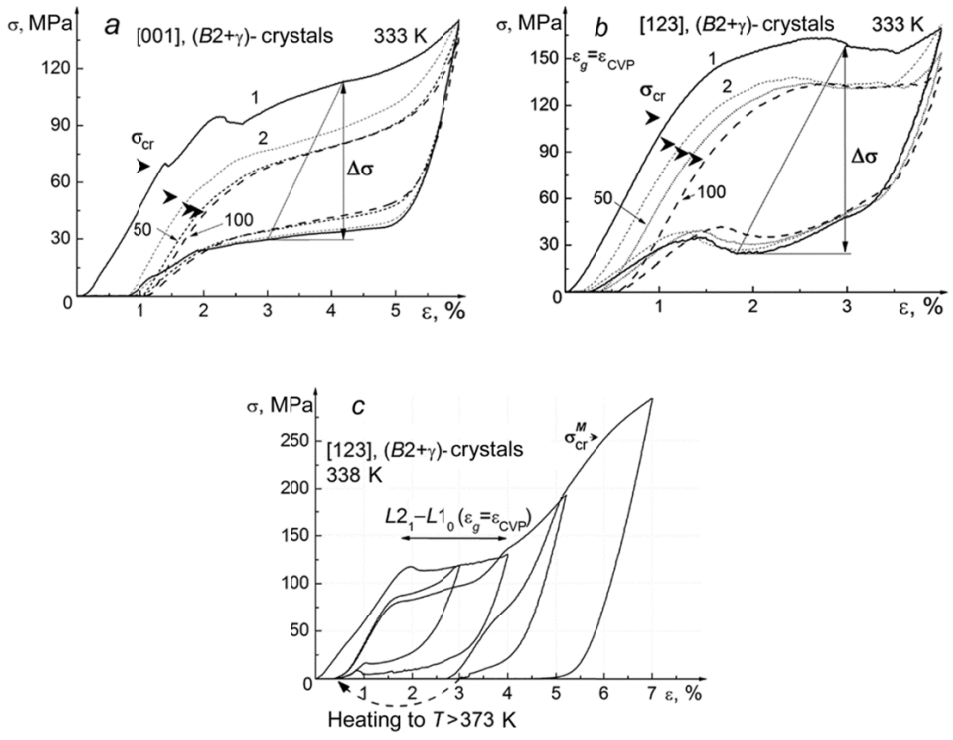

Fig. 5. Results of cycling of quenched heterophase ($B2+\gamma$)-crystals of $Ni_{49}Fe_{18}Ga_{27}Co_6$ alloy at $T = 333–338$ K: [123]-orientation (a), [001]-orientation (b), σ(ε) response during the investigation of the martensite yield stress in ($B2+\gamma$)-crystals oriented along the [123]-direction.

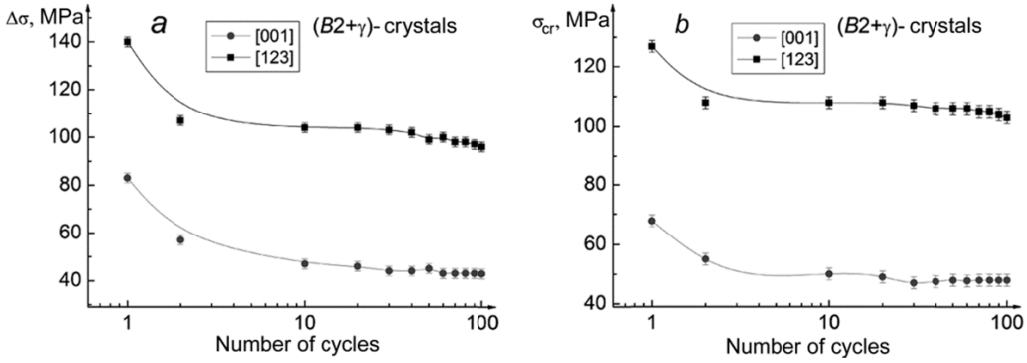

Fig. 6. Dependence of stress hysteresis Δσ (*a*) and critical stresses of martensite formation σ_{cr} (*b*) on the number of loading/unloading cycles for ($B2+\gamma$)-crystals of $Ni_{49}Fe_{18}Ga_{27}Co_6$ alloy.

variant martensite structure is formed (Fig. 7). This gives rise to a situation, where in ($B2+\gamma$)-crystals oriented along [001]- and [123]-directions the transformation, taking place under the same thermodynamic conditions (i.e., at $T = A_f$ + (12–15) K), is characterized by higher critical stresses of martensite $\sigma_{cr} \sim 50$ and 110 MPa and wider hysteresises, $\Delta\sigma \sim 50$ and 110 MPa, respectively, in contrast to $L2_1$ crystals (Fig. 5). In [123]-oriented crystals with ($B2+\gamma$)-structure, the hysteresis strongly depends on the given strain ε_g and at $\varepsilon_g > 4\%$ Δσ increases to such an extent that the specimen dimensions are recovered after heating to $T > 373$ K only (Fig. 5*c*), i.e., a stabilization of stress-induced $L1_0$-martensite is observed (Fig. 5*c*). In both orientations of ($B2+\gamma$)-crystals at $\varepsilon_g = \varepsilon_{CVP}(L1_0)$, where detwinning of $L1_0$-martensite does

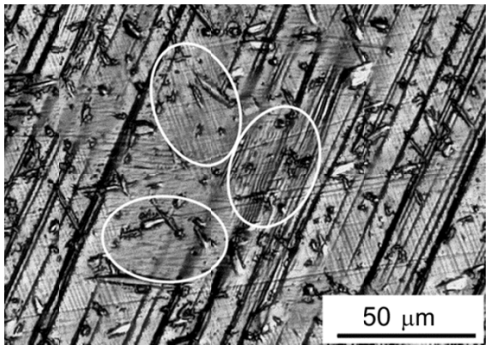

Fig. 7. Optical metallography of the surface ($B2+\gamma$)-single crystals of $Ni_{49}Fe_{18}Ga_{27}Co_6$ alloy after 100 loading/unloading cycles; the ovals outline different martensite variants.

not contribute to transformation strain, cyclic stability of SE slightly depends on orientation (Fig. 5), similarly to $L2_1$-crystals. On the other hand, the changes in morphology of stress-induced martensite and in the sequence of MTs in ($B2+\gamma$)-crystals, compared to $L2_1$-crystals, result in dramatic degradation of SE even without any detwinning of $L1_0$-martensite: the value of critical stress σ_{cr} for either orientation of quenched crystals is reduced by 20–27%, and the value of stress hysteresis $\Delta\sigma$ – by 32–47% (Fig. 5 and 6).

It is evident from Figs. 1 and 5 that in all structural states and orientations of the crystals (except for high-strength [001]-oriented crystals with $L2_1$-structure) the degradation of SE is achieved after the first loading/unloading cycle – decreased martensite formation stresses σ_{cr}, reduced stress hysteresis value $\Delta\sigma$ and different shape of the $\sigma(\varepsilon)$ curves (Figs. 1 and 5). Such SE degradation is observed after the first cycle in practically all shape memory alloys [15, 16]. A sharp reduction in the stresses in the second loading/unloading cycle is generally attributed to the formation of dislocations and martensite crystals after the first cycle, which in subsequent cycles facilitate the nucleation of martensite. In the case of high-strength crystals, the austenitic and martensitic phases demonstrate high resistance to the formation of dislocations, in other words, the effect of the first cycle (sharp decrease in σ_{cr} and $\Delta\sigma$) is not observed, which was experimentally proved for high-strength [001]-oriented crystals with $L2_1$-structure. In the ($B2+\gamma$)-heterophase crystals, a stronger decrease in σ_{cr} after the first cycle, compared to $L2_1$-crystals, is associated with the formation of dislocations and residual martensite near the γ-particle – $B2$-matrix interface, which is accompanied by irreversible strain in the first cycle up to $\varepsilon_{irr} = 0.7\%$.

In the general case, in crystals with thermoelastic MTs we can single out the following principal mechanisms of degradation of functional properties during cyclic loading [15]: presence of residual martensite and dislocation slip during stress-induced MTs. These processes give rise to a high level of energy dissipation ΔG_{irr} during transformation, which is characterized by stress hysteresis. It was assumed in [15, 17, and 18] that cyclic stability of SE could be predicted relying on the value of stress hysteresis $\Delta\sigma$ in the first loading/unloading cycle: the narrower is the hysteresis $\Delta\sigma$, the higher would be the stability of material to cyclic loading. We show here that it is not always possible to describe the dependence of cyclic stability on orientation or microstructure using the dissipated energy value only. Firstly, single-phase single crystals with $L2_1$-structure in the absence of detwinning ($\varepsilon_g = 3.5\% \sim \varepsilon_{CVP}(L1_0)$ for [123]-oriented rystals) demonstrate high cyclic stability of SE, while the value of stress hysteresis in [123]-oriented crystals ($\Delta\sigma \sim 50$ MPa) is by a factor of 4 higher than that in [001]-oriented crystals ($\Delta\sigma = 12$ MPa). Secondly, the values of $\Delta\sigma$ in [123]-oriented crystals with $L2_1$-structure for the case of given strain value $\varepsilon_g = 3.5\% \sim \varepsilon_{CVP}(L1_0)$ and in [001]-oriented crystals with ($B2+\gamma$)-structure are similar $\Delta\sigma \approx 50$ MPa, but in ($B2+\gamma$)-crystals, a higher degradation of SE is observed compared to $L2_1$-crystals. Therefore, in order to predict cyclic stability of SE, in this work we propose to use the ratio of the reversible (elastic +surface) energy ΔG_{rev} to the dissipated energy ΔG_{irr} during stress-induced MTs. Table 2 presents the values of ΔG_{rev} and ΔG_{irr} per unit volume calculated in the first loading/unloading cycle inside the $\sigma(\varepsilon)$ curve and the area below the unloading curve, respectively [19]. This ratio characterizes the relationship between critical stresses σ_{cr}, stress hysteresis $\Delta\sigma$, and reversible ε_{rev} and irreversible ε_{irr} strains. In the [001]- and [123]-oriented single crystals with $L2_1$-structure during the formation of stress-induced 14M-martensite and in the absence of

TABLE 2. Elastic and Dissipated Energies Calculated in the First Cycle σ(ε) in (*B*2+γ)- and *L*2$_1$- $Ni_{49}Fe_{18}Ga_{27}Co_6$ Crystals

Crystal structure	*L*2$_1$-single crystals			(*B*2+γ)-single crystals	
Orientation	[123]		[001]	[123]	[001]
Value of ε_g	$\varepsilon_g = 3.5\% \sim \varepsilon_{CVP}$	$\varepsilon_g = 5.5\% \sim \varepsilon_{CVP+detw}$	$\varepsilon_g = 6\% \sim \varepsilon_{CVP}$	$\varepsilon_g = 4\% \sim \varepsilon_{CVP}$	$\varepsilon_g = 6\% \sim \varepsilon_{CVP}$
ΔG_{rev}, MJ/m^3	2.0	1.6	1.4	1.6	1.8
ΔG_{irr}, MJ/m^3	1.2	3.2	0.8	3.4	3.5
$\Delta G_{rev}/\Delta G_{irr}$	1.7	0.5	1.8	0.5	0.5

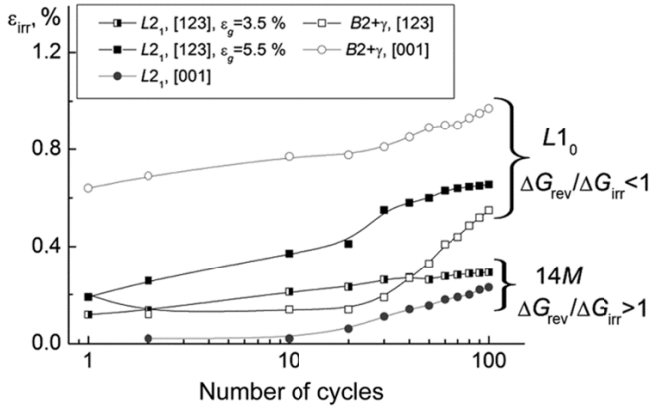

Fig. 8. Dependence of residual deformation ε_{irr} on the number of loading/unloading cycles increasing within 1–100 for the initial and quenched [123]- and [001]-oriented single crystals of $Ni_{49}Fe_{18}Ga_{27}Co_6$ alloy in compression.

detwinning ($\varepsilon_g = 3.5\%$) the reversible energy ΔG_{rev} is by a factor of 1.5 higher than the energy dissipated ΔG_{irr} ($\Delta G_{rev}/\Delta G_{irr} > 1.0$) and their ratio $\Delta G_{rev}/\Delta G_{irr}$ for both orientations is found to be 1.7–1.8 (Table 2).

A large part of the stored reversible energy ΔG_{rev}, which is the driving force of the reverse MT, gives rise to a high cyclic stability of SE and its weak dependence on orientation in *L*2$_1$-crystals (Fig. 1 and 6). In this case, the storage of residual irreversible strain during the entire 100 loading/unloading cycles (*L*2$_1$-structure for $\varepsilon_g = \varepsilon_{CVP}$) is less than 0.2%, irrespective of orientation (Fig. 8). In *L*2$_1$-crystals oriented along the [123]-direction with a complete sequence of *L*2$_1$–14*M*–*L*1$_0$-MTs and detwinning of *L*1$_0$-martensite ($\varepsilon_g = 5.5\% \sim \varepsilon_{CVP+detw}(L1_0)$, on the contrary, the dissipated energy ΔG_{irr} is twice higher than the reversible energy ΔG_{rev} ($\Delta G_{rev}/\Delta G_{irr} = 0.5 < 1$), and the irreversible energy is found to be 0.65%. The principal physical reason for an increase in energy dissipation with the number of cycles in single-phase *L*2$_1$crystals is detwinning of the crystals of *L*1$_0$-martensite, which results in movement of the habitus plane from its invariant position under the action of external stress and generation of additional internal stresses, which is detailed in [10, 11]. The relaxation of these internal stresses near the phase- and twin boundaries due to dislocation slip at a low martensite strength yield level ($\sigma_{cr}^{M} = 270$ MPa), favors the development of reversible MTs with a wide stress hysteresis $\Delta\sigma = 100$ MPa and determines considerable degradation of SE along the [123]-direction for the given strain being ($\varepsilon_g = 5.5\% \sim \varepsilon_{CVP+detw}$).

In (*B*2+γ)heterophase crystals, nucleation and interaction of multiple variants of *L*1$_0$-martensite due to the presence of γ-phase particles results in increased dissipated energy ΔG_{irr}, whose value is twice higher than that of the stored reversible energy ΔG_{rev} (Table 2) even at $\varepsilon_g = \varepsilon_{CVP}(L1_0)$ in the absence of detwinning, and there is considerable degradation of SE with irreversible strain up to 1.0% as the number of cycles increases from 1 to 100 (Fig. 8).

SUMMARY

The influence of crystal structure of stress-induced martensite (14*M* or$L1_0$), detwinning of $L1_0$-martensite crystals, strength properties of austenite and martensite, as well as γ-phase particles measuring 5–10 μm on cyclic stability of SE under conditions of thermal loading/unloading cycling (1 to 100 cycles) in [001]- and [123]-oriented single crystals of $Ni_{49}Fe_{18}Ga_{27}Co_6$ (at.%) alloy in single-phase ($L2_1$) and heterophase ($B2+\gamma$) states at the temperature $T = A_f+(12–15)$ K has been experimentally determined.

Single-phase $L2_1$-single crystals oriented along [001]-direction exhibit the highest cyclic stability of SE: as the number of cycles increases from 1 to 100, the irreversible strain is as low as 0.2%, and the values of critical stress σ_{cr} and stress hysteresis $\Delta\sigma$ remain constant within the measurement error 5%. The physical reasons for high stability of these crystals to cyclic degradation are as follows: 1) high strength properties of $L2_1$-austenite (σ_{cr}^{A} = 1000 MPa) and 14*M*-martensite (σ_{cr}^{M} = 1680 МПа); 2) low energy dissipation and hence narrow stress hysteresis ($\Delta\sigma$ = 12 MPa), which is controlled by high mobility of the phase boundary during the development of $L2_1$–14*M*-transformation and the absence of a contribution from detwinning of the martensite crystals.

In low-strength, one-phase $L2_1$ single crystals oriented along [123]-direction, during the development of $L2_1$–14*M*–$L1_0$-MT followed by detwinning of $L1_0$-martensite crystals (ε_g = 5.5% ~ $\varepsilon_{CVP+detw}(L1_0)$) a severe degradation of SE is observed: as the number of cycles is increased, the irreversible strain increases up to 0.7% and the values of σ_{cr} and $\Delta\sigma$ decrease by 25 and 30%, respectively. This behavior is dictated by: 1) low strength properties of $L1_0$-martensite (σ_{cr}^{M} = 270 MPa; 2) large value of energy dissipation and hence a wide stress hysteresis $\Delta\sigma$ = 100 MPa, which is associated with low mobility of the phase boundary during the development of $L2_1$–14*M*–$L1_0$-transformation due to the distorted invariant position of the habitus plane in the course of detwinning of $L1_0$-martensite crystals. In the cases where the given strain in [123]-oriented crystals is small and there is no martensite detwinning at ε_g = 3.5% ~ $\varepsilon_{CVP+detw}(14M) = \varepsilon_{CVP}(L1_0)$, the value of stress hysteresis is reduced by a factor of 2 ($\Delta\sigma$ = 50 MPa), and SE is more stable.

The cyclic stability of SE in ($B2+\gamma$) heterophase single crystals of $Ni_{49}Fe_{18}Ga_{27}Co_6$ alloy during the development of $B2$–$L1_0$-MTs and in the absence of detwinning of $L1_0$-crystals under loading $\varepsilon_g = \varepsilon_{CVP}(L1_0)$ has been observed to decrease compared with single-phase $L2_1$ single crystals. This is controlled by the changed morphology of $L1_0$-martensite crystals and the multivariant character of MT via the prevailing nucleation of martensite crystals near the particle–matrix boundary.

In this work, a method for predicting cyclic stability of SE from the ratio between the reversible ΔG_{rev} and dissipated ΔG_{irr} energies during the development of a stress-induced MT has been proposed. In $L2_1$-single crystals of $Ni_{49}Fe_{18}Ga_{27}Co_6$ alloy in single-phase state, an $L2_1$–14*M* stress-induced transformation is characterized by a high level of reversible energy ΔG_{rev}, which exceeds that of the dissipated energy ΔG_{irr}, and represents a driving force of the reverse MT ($\Delta G_{rev}/\Delta G_{irr}$ = 1.7–1.8), which favors high cyclic stability of SE. During the development of $L2_1$–14*M*–$L1_0$-MTs in [123]-oriented single-phase crystals and $B2$–$L1_0$-MTs in ($B2+\gamma$)-heterophase single crystals, the ratio between the reversible and dissipated energies is smaller than unity $\Delta G_{rev}/\Delta G_{irr}$ = 0.5, and these crystals demonstrate a low cyclic stability of superelasticity.

This study has been supported by the Russian Science Foundation, Grant No. 16-19-10250.

REFERENCES

1. H. E. Karaca, I. Karaman, B. Basaran, *et al*., Acta Mater., **54**, 233–245 (2006).
2. H. Morito, A. Fujita , K. Oikawa, *et al*., Appl. Phys. Lett., **90**, 062505 (2007).
3. E. Panchenko, Y. Chumlyakov, H. J. Maier, *et al*., Intermetallics, **18**, 2458–2463 (2010).
4. P. Mullner, V. A. Chernenko, and G. Kostorz, J. Appl. Phys., **95**, 1531–1536 (2004).
5. C. Efstathiou, H. Sehitoglu, P. Kurath, *et al*., Scripta Mater., **57**, 409–412 (2007).
6. E. Yu. Panchenko, Yu. I. Chumlyakov, E. E. Timofeeva, *et al*., Russ. Phys. J., 55, No. 9, 1046–1051 (2013).
7. R. F. Hamilton, H. Sehitoglu, C. Efstathio, and H. J. Maier, Acta Mater., **55**, 4867–4876 (2007).
8. J. Liu, N. Scheerbaum, D. Hinz, and O. Gutfleisch, Acta Mater., **56**, 3177–3186 (2008).

9. E. E. Timofeeva, E. Yu. Panchenko, Yu. I. Chumlyakov, *et al*., Mater. Sci. Eng. A, **640**, 465–470 (2015).
10. A. L. Roytburd and Ju. Slusker, Mater. Sci. Eng. A, **238**, 23–31 (1997).
11. A. L. Roytburd, Mater. Sci. Forum., **327**–**328**, 389–392 (2000).
12. C. Efstathiou, H. Sehitoglu, J. Carroll, *et al*., Acta Mater., **56**, 3791–3799 (2008).
13. E. E. Timofeeva, E. Yu. Panchenko, Yu. I. Chumlyakov, and A. I. Tagiltsev, Russ. Phys. J., **57**, No. 9, 1268–1277 (2015).
14. Yu. I. Chumlyakov, I. V. Kireeva, E. Yu. Panchenko, *et al*., 54, No. 8, 937–950 (2012).
15. K. Gall and H. Maier, Acta Mater., **50**, 4643–4657 (2002).
16. C. Yu, G. Kang, and Q. Kan, Mech. Phys. Solids, **82**, 97–136 (2015).
17. Y. Liu, I. Houver, H. Xiang, *et al*., Metallurg. Mater. Trans. A, **30A**, 1275–1282 (1999).
18. J. Dadda, H. J. Maier, D. Niklasch, *et al*., Metallurg. Mater. Trans. A, **39A**, 2026–2039 (2008).
19. E. Pieczyska, S. Gadaj, W. K. Nowacki, *et al*., Sci. Technol. Adv. Mater., **6**, 889–894 (2005).